Aspartate 75 Mutation in Sensory Rhodopsin II from *Natronobacterium pharaonis* Does Not Influence the Production of the K-Like Intermediate, but Strongly Affects Its Relaxation Pathway

Aba Losi,* Ansgar A. Wegener,† Martin Engelhard,† Wolfgang Gärtner,* and Silvia E. Braslavsky*

*Max-Planck-Institut für Strahlenchemie, Postfach 10-13-65, D-45413 Mülheim an der Ruhr, and †Max-Planck-Institut für molekulare Physiologie, Rheinlanddamm 201, D-44139 Dortmund, Germany

ABSTRACT The early steps in the photocycle of the aspartate 75-mutated sensory rhodopsin II from *Natrobacterium pharaonis* (pSRII-D75N) were studied by time-resolved laser-induced optoacoustic spectroscopy combined with quantum yield determinations by flash photolysis with optical detection. Similar to the case of pSRII-WT, excitation of pSRII-D75N produces in subnanosecond time a K-like intermediate. Different to the case of K in pSRII-WT, in pSRII-D75N there are two K states. K_E decays into K_L with a lifetime of 400 ns (independent of temperature in the range 6.5–52°C) which is optically silent under the experimental conditions of our transient absorption experiments. This decay is concomitant with an expansion of 6.5 ml/mol of produced intermediate. This indicates a protein relaxation not affecting the chromophore absorption. For pSRII-D75N reconstituted into polar lipids from purple membrane, the mutation of Asp-75 by the neutral residue Asn affects neither the K_E production yield (Φ_{K_e} 0.51 ± 0.05) nor the energy stored by this intermediate ($E_{E^{K_E}}$ = 91 ± 11 kJ/mol), nor the expansion upon its production ($\Delta V_{R,1}$ = 10 ± 0.3 ml/mol). All these values are very similar to those previously determined for K with pSRII-WT in the same medium. The millisecond transient species is attributed to K_L with a lifetime corresponding to that determined by electronic absorption spectroscopy for K_{565}. The determined energy content of the intermediates as well as the structural volume changes for the various steps afford the calculation of the free energy profile of the phototransformation during the pSRII-D75N photocycle. These data offer insights regarding the photocycle in pSRII-WT. Detergent solubilization of pSRII-D75N affects the sample properties to a larger extent than in the case of pSRII-WT.

INTRODUCTION

The *cis-trans* photoisomerization of the chromophore in retinal proteins triggers a series of protein conformational changes responsible for the specific function of the protein. The earliest event in the photocycle (comprising the chromophore isomerization) eventually leads, in the subnanosecond time range, to the formation of a red-shifted intermediate, which, in the light-driven proton pump BR, is called the K intermediate. (Oesterhelt, 1998, and references therein). By analogy, in the sensory rhodopsins the few-microsecond transient species is denominated the K-like intermediate.

The major conformational changes of the retinal proteins occur in the millisecond to seconds timescale and little is known regarding how the subnanosecond conformational changes of the K (or K-like) intermediate drive the functional processes (Oesterhelt, 1998). The information about how the protein responds to the motion of the chromophore is also sparse. FTIR experiments have revealed that, concomitant with the geometric rearrangements of the chromophore, changes in the protein skeleton occur as early as upon formation of the red-shifted intermediate (Edman et al., 1999; Siebert, 1995). Movements of the main-chain Lys 216 have been recently observed by high-resolution x-ray analysis of the low-temperature K intermediate in BR (Edman et al., 1999). Moreover, step scan FTIR studies with BR have revealed the presence of two K substates, i.e., an early K_E and a late K_L, the latter having a lifetime corresponding to the decay of the one detected by time-resolved electronic absorption, K_{590}. (Dioumaev and Braiman, 1997; Hage et al., 1996; Weidlich and Siebert, 1993).

Accordingly, all retinal proteins so far investigated exhibit protein movements accompanying the early steps of the photocycle, which can be detected as structural volume changes ($\Delta V_{R,i}$) by means of LIOAS (Gensch et al., 1998; Losi et al., 1999a; Zhang and Mauzerall, 1996).

Although a quantitative correlation between the changes detected by FTIR and LIOAS techniques has not yet been established, an interesting observation was made during the study of pSRII, an archeal retinal-containing photosensor. FTIR measurements on the K-like intermediate from pSRII have demonstrated the occurrence of relatively large protein conformational changes as compared to other retinal proteins (Engelhard et al., 1996). In line with these observations, a value of $\Delta V_{R,K}$ = +10 ml/mol was determined by LIOAS (Losi et al., 1999b), so far the largest value mea-

Received for publication 8 November 1999 and in final form 26 January 2000.

Address reprint requests to Silvia E. Baslavsky, Max-Planck-Institut für Strahlenchemie, Stiftstrasse 34–36, D-45470 Mülheim an der Ruhr, Germany. Tel.: +49-208-306-3681; Fax: +49-208-306-3951; E-mail: braslavskys@mpi-muelheim.mpg.de.

Dr. Losi's present address is Istituto Nazionale per la Fisica della Materia, Parco Area delle Scienze 7/A, 43100 Parma, Italy.

Abbreviations used: BR, bacteriorhodopsin; DM, *n*-dodecyl-β-D-maltoside; FTIR, Fourier-transform infrared; LIOAS, laser-induced optoacoustic spectroscopy; pSRII, sensory rhodopsin II from *Natronobacterium pharaonis*; PML, polar lipids from purple membrane; SB, Schiff base.

0006-3495/00/05/2581/09 $2.00

sured for this step in a retinal protein. This result strongly indicates that the $\Delta V_{R,K}$ value reflects changes in the protein skeleton. Other sources of volume changes may be small intrinsic geometrical rearrangements of the chromophore (Edman et al., 1999) and modifications of weak interactions within the retinal cavity. In this early step of the photocycle, solvation effects are likely to be small due to the inaccessibility of the retinal cavity as has been confirmed for pSRII (Losi et al., 1999b) and for BR (Zhang and Mauzerall, 1996).

The origin of $\Delta V_{R,i}$ for the various steps in the photocycle, and the relative weight of different contributions may be partially elucidated by studying proteins mutated in residues that are part of the retinal cavity. Polar or ionized amino acids are of special interest because they take part in hydrogen-bond network and in electrostatic interactions within the retinal cavity (Oesterhelt, 1998, and references therein) and they could be crucial for the stereodynamical course of the chromophore changes (Humphrey et al., 1997).

Mutations in the BR-active site have highlighted the role of Asp-85 as the proton acceptor, following the deprotonation of the retinal SB. Asp-85 is negatively charged in ground state BR and is part of the complex counterion of the protonated SB (Subramaniam et al., 1992). The corresponding residue in pSRII, Asp-75, is also ionized in the parent state and, most probably, can be identified with the carboxylate group that becomes protonated during the formation of the long-lived M state, which contains a deprotonated SB (Engelhard et al., 1996). Removal of the Asp negative charge by site-directed mutagenesis in both photoreceptors (pSRII-D75N and BR-D85N) deeply affects the respective photocycle (Schmies et al., 2000; Mogi et al., 1988).

In sensory rhodopsin II from *Halobacterium salinarum*, hSRII, it has also been demonstrated that the corresponding Asp-73 is a counteranion to the protonated SB (Zhu et al., 1997) and serves as the proton acceptor from the SB during the photoconversion to the M state. Additionally, cells carrying the hSRII-D73N mutation, exhibit a strongly reduced light response and do not form the M intermediate (Spudich et al., 1997). Asp-75 in pSRII and Asp-73 in hSRII should thus be functionally and structurally related to Asp-85.

On the contrary, in the positive phototaxis receptor sensory rhodopsin I (SRI), the corresponding Asp-76 is protonated in the parent state and does not undergo protonation changes during the photocycle. The mutation D76N does not alter the pattern of charges around the SB and, consequently, is functionally inactive, i.e., the long-lived M-like intermediate is still formed (Rath et al., 1994). Deprotonation of Asp-76 at pH $>$ 7 renders SRI into a light-driven proton pump, where Asp-76 is now the proton acceptor (Bogomolni et al., 1994; Haupts et al., 1996).

We have previously shown that the mutation D76N in SRI does not markedly alter either the quantum yield of the retinal photoisomerization nor the energy content of the K-like intermediate, S_{610}, though the total efficiency of the photocycle is much lower in SRI-D76N (Losi et al., 1999a; Rath et al., 1994). Yet, the first steps of the photocycle are somehow affected by the mutation, i.e., the formation of S_{610} is accompanied by a ΔV_R that is much smaller in SRI-D76N than in SRI-WT (1.5 versus 5.5 ml/mol), the S_{610} decay to the subsequent intermediate occurs with a lower activation energy (41 kJ/mol versus 67 kJ/mol) compensated somehow by a smaller preexponential factor (1.6×10^{13} s^{-1} versus 3×10^{17} s^{-1} (Losi et al., 1999a) indicating a larger rigidity of the retinal cavity in SRI-WT.

We present in this report the results of time-resolved LIOAS studies with the mutated protein pSRII-D75N, combined with quantum yield determinations by flash photolysis with optical detection. In addition to $\Delta V_{R,i}$, LIOAS supplies the values of the energy stored by the first intermediates in the photocycles (Schulenberg and Braslavsky, 1997).

The LIOAS experiments evidence the occurrence of an otherwise optically silent decay with a lifetime of hundreds of nanoseconds, indicating that the energy-rich K_E, formed in the subnanosecond time range, decays following a biphasic kinetics. The transient with an ~400-nanoseconds lifetime should be related to protein relaxation, whereas the isomerized chromophore thermally returns to the ground state in milliseconds (K_L), as determined by flash photolysis. The comparison of the LIOAS results with step-scan FTIR data on BR offer hints for understanding the origin of the molecular volume changes occurring in the early stages of the pSRII photocycle and are discussed in terms of the differences and similarities between pSRII, SRI, and BR.

EXPERIMENTAL PROCEDURES

Protein expression and purification

pSRII-D75N was expressed as described by Schmies et al. (2000). Further purification and assembly were carried out as described by Losi et al. (1999b). Measurements were performed either with pSRII in 25 mM sodium phosphate buffer pH = 8 with *n*-dodecyl-β-D-maltoside (DM) = 0.025%, or with pSRII in polar PML lipids in 25 mM sodium phosphate, pH = 8. The absorbances used were 0.2 (at 532 nm) for flash photolysis and ~0.1.

Instrumentation

Absorption spectra were recorded with a UV-2102PC spectrophotometer (Shimadzu Germany, Duisburg, Germany). Steady-state fluorescence measurements were performed with a Spex Fluorolog spectrofluorometer. Cresyl violet (Lambda PhysiK GmbH, Göttingen, Germany) was used as a fluorescence reference (Φ_F = 0.54 in methanol [Losi et al., 1999b]). The area of the emission spectra of solutions of sample and reference at matched absorbance (~0.05) at the

excitation wavelength were used for the calculation of the emission quantum yield.

For the LIOAS experiments, excitation at 500 nm was achieved by pumping the frequency-tripled pulse of a Nd:YAG laser (SL 456G, 6-ns pulse duration, 355 nm, Spectron Laser System, Rugby, Great Britain) into a Beta Barium Borate Optical Parametric Oscillator (OPO-C-355, bandwidth 420–515 nm, Laser Technik Vertriebs GmbH, Ertestadt-Friesheim, Germany). A frequency doubled Nd:YAG laser was used for excitation at 532 nm (SL802, 11-ns pulse, Spectron Laser Systems). Reference and sample absorbances were matched within 5% at the excitation wavelength. The beam was shaped by a slit (0.5 × 6 mm), which determines an acoustic transit time in aqueous solution of about 300 ns (Braslavsky and Heibel, 1992) allowing a time resolution of ~30 ns by using deconvolution techniques (Rudzki et al., 1985). Special care was taken to perform the experiments in the linear regime of amplitude versus laser fluence, which was up to 30 μJ/pulse. The total incident energy normally used was ~10 μJ/pulse (fluence = 330 μJ/cm^2).

The thermoelastic parameters of the buffers were determined by comparison to those of pure water, as previously described (Losi et al., 1999a). Evans blue and bromocresol green (Sigma Chemical Co., St. Louis MO) were used as calorimetric reference compounds in neat water and in the buffer solutions, respectively. The concentration of DM was matched between the sample and reference preparations.

The time evolution of the pressure wave was assumed to be a sum of monoexponential functions. This function has proven to fit the decays of all other photoreceptors studied by LIOAS to date (Schulenberg and Braslavsky, 1997). The deconvolution analysis yielded the fractional amplitudes (φ_i) and the lifetimes (τ_i) of the transients (Sound Analysis 3000, Quantum Northwest Inc., Spokane, WA). The time window was between 10 ns and 5 μs; decays faster than 10 ns were integrated by the piezoelectric transducer, whereas decays longer than 5 μs were not sensed.

Eq. 1 was used to separate heat release, q_i, and structural volume changes, $\Delta V_{r,i}$. Both effects contribute to the amplitudes, φ_i, recovered from deconvolution (Rudzki-Small et al., 1992; Rudzki et al., 1985).

$$\varphi_i = \frac{q_i}{E_\lambda} + \frac{\Delta V_{r,i}}{E_\lambda}\frac{c_p\rho}{\beta}, \qquad (1)$$

where E_λ is the molar excitation energy, $\beta = (\partial V/\partial T)_p \cdot (1/V)$ is the volume expansion coefficient, c_p is the heat capacity at constant pressure, and ρ is the mass density of the solvent. $\Delta V_{r,i} = \Phi_i \Delta V_{R,i}$, where Φ_i is quantum yield of the ith process and $\Delta V_{R,i}$ is the structural volume change per mol of phototransformed species. The variation in the ratio of thermoelastic parameters ($c_p\rho/\beta$) was achieved by varying the temperature, according to the "several temperatures (ST) method" (van Brederode et al., 1995). The fraction of absorbed energy released as heat in the ith step, $\alpha_{thi} = q_i/E_\lambda$ 12, is then recovered from the intercept and $\Delta V_{r,i}$ from the slope of the plots φ_i versus ($c_p\rho/\beta$), provided that both parameters remain constant over the temperature range used.

Flash photolysis measurements were performed with the equipment already described by Ruddat et al. (1997) using 532-nm excitation, as in the LIOAS experiments. 5,10,15,20-Tetrakis-(4-sulphonatophenyl)-porphin (TPPS) (Porphyrin Products Inc. Logan, UT) was used as an actinometer (van Brederode et al., 1995).

For the titrations, the pH was varied by adding small amounts of 1 M NaOH. The pH was measured by means of a Basic pH Meter (Denver Instrument Co., Arvada, CO), equipped with an Inlab 423 electrode for the direct monitoring of the pH in the cuvette.

RESULTS

The pK$_a$ of the Schiff base

The pH titration of pSRII-D75N shows a curve with two inflection points (Fig. 1). In PML, the two pK$_a$ values are readily determined and the curve was fitted with Eq. 2, derived from the Henderson-Hasselbalch equation,

$$a = a_0 + (a_1 - a_0) \times \frac{10^{n_1(pH-pK_{a1})}}{1 + 10^{n_1(pH-pK_{a1})}} + (a_2 - a_1) \times \frac{10^{n_2(pH-pK_{a2})}}{1 + 10^{n_2(pH-pK_{a2})}}, \qquad (2)$$

where a is any observable (in this case the variation of a particular absorption band), and n_1 and n_2 are empirical parameters describing the cooperativity of the proton association (Hill index).

The first equilibrium with pK$_a$ = 10.5 has a Hill index n = 2.1 ± 0.6, whereas the second pK$_a$ = 12.2 displays a larger cooperativity degree (n = 3.1 ± 0.9) (Fig. 1) and the reaction at this high pH is not completely reversible. The first equilibrium with pK$_a$ = 9 in DM solutions has instead, a large Hill index (n = 6.5 ± 3.9) whereas the second pK$_a$ = 10.05 corresponds to a single proton release (n = 1.1 ± 0.4). The thermochromic spectral equilibrium in DM is thus most probably related to the pH of the buffer being relatively close to the first dissociation of the SB. Increasing the pH above 10 in the DM samples, produces irreversible changes in the spectrum. The strong increase in scattering indicates that the protein becomes denatured and a correction for this effect is required to correctly interpret the titration data. Contrary to the PML preparations, in DM at pH ≥ 12, the protein appears to be completely denatured and precipitation occurs giving rise to highly scattering solutions.

In view of the complexity of the system and the relatively high buffer concentrations needed to stabilize the protein, it

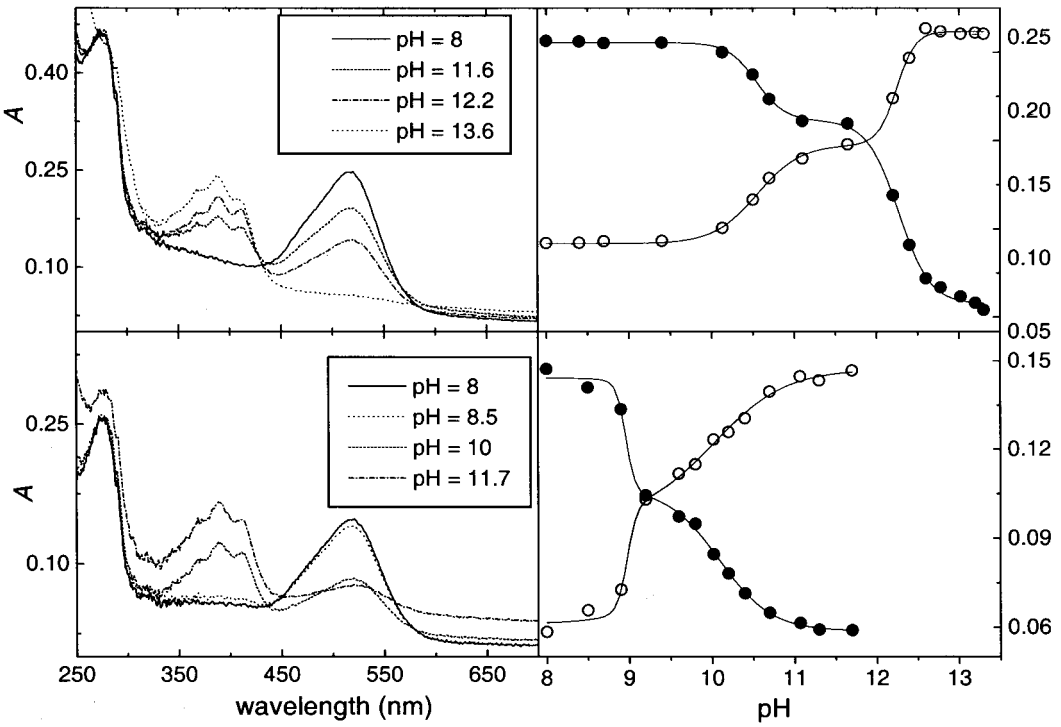

FIGURE 1 pH Titration of pSRII-D75N in (*top*) PML 20:1 and (*bottom*) DM. The titration curves were built by using the absorption at (●) 520 and (○) 390 nm as parameters. The increasing of the band at 390 nm indicates the appearance of the deprotonated SB. The experimental data points were fitted using Eq. 2.

is very difficult to interpret the high values of the Hill indices and to assign the pK_a values to a particular equilibrium.

LIOAS of PML-reconstituted protein

For the PML-reconstituted pSRII-D75N, the $(c_p\rho/\beta)$-dependent plots of the amplitudes recovered from deconvolution of the signal and corresponding to the lifetime $\tau_1 < 10$ ns, yielded results similar to those for the wild type (WT) protein (Table 1). An expansion of $\Delta V_{r,1} = 5$ ml/mol accompanies this fast step. Taking the quantum yield of K formation, $\Phi_K = 0.5$ (see below), a molar value $\Delta V_{R,1} = (10 \pm 1.5)$ ml/mol is obtained. The energy content of the first intermediate (K-like, corresponding to K_E, see above) is calculated as $E_{KE} = (91 \pm 11)$ kJ/mol by using Eq. 3, derived from simple energy-balance considerations and neglecting fluorescence (see below):

$$\alpha_{th1} = 1 - \Phi_K \frac{E_{K_E}}{E_\lambda}. \quad (3)$$

A sum of two single-exponential functions was required for the fitting of the LIOAS waveforms (Fig. 2) at all the temperatures used. The decay following the prompt pulse was not thermally activated within the temperature range 7–50°C and the lifetime associated with it was $\tau_2 = (400 \pm 120)$ ns (see Fig. 3). An average expansion of $\Delta V_{r,2} = (3.3 \pm 0.25)$ ml/mol is associated with this decay. Because

TABLE 1 LIOAS parameters for the formation of K_E in pSRII-D75N as compared to the data for K in pSRII-WT.

	pSRII-D75N				pSRII-WT*		
	λ_{exc} (nm)	α_{th1} ($\tau_1 < 10$ ns)	$\Delta V_{r,1}$† (ml/mol)	$\Delta V_{R,1}$‡ (ml/mol)	α_{th1} ($\tau_1 < 10$ ns)	$\Delta V_{r,1}$† (ml/mol)	$\Delta V_{R,1}$‡ (ml/mol)
PML§ 20:1	532	0.77 ± 0.04	5.2 ± 0.3	10.2 ± 1.6			
PML 20:1	500	0.85 ± 0.03	5 ± 0.1	9.8 ± 1.1	0.79 ± 0.05	4.8 ± 0.2	9.4 ± 1.3
PML 100:1	500	0.80 ± 0.03	4.9 ± 0.3	9.6 ± 1.5	0.79 ± 0.04	4.4 ± 0.2	8.6 ± 1.2
DM	532	1 ± 0.05	5.2 ± 0.2	10.2 ± 1.4	0.82 ± 0.04	5.1 ± 1	10 ± 3

*Losi et al. (1999b).
†Measured values. In every case the regression value of the linear fitting was $r > 0.990$.
‡Molar structural volume change calculated using $\Delta V_{r,i}$ and the quantum yields, as $\Delta V_{r,i}/\Phi_i$ and considering the relative errors.
§For the PML samples the lipid-to-protein ratio is indicated.

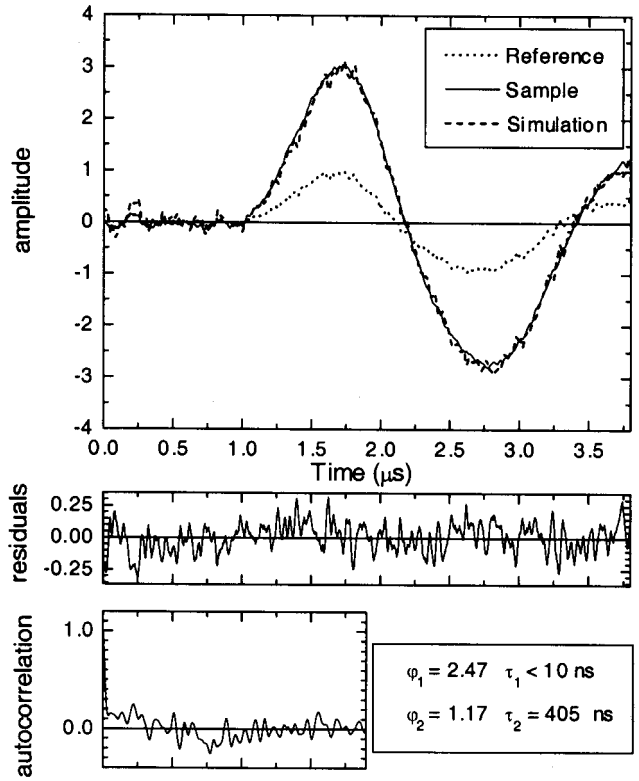

FIGURE 2 LIOAS signal for pSRII-D75N in PML 20:1 at $T = 6.5°C$, $\lambda_{exc} = 532$ nm. *Inset*: deconvolution results. At this relatively low temperature, the two consecutive expansions accompanying the formation and decay of K_E are the main contributions to the signal. Reference: bromocresol green.

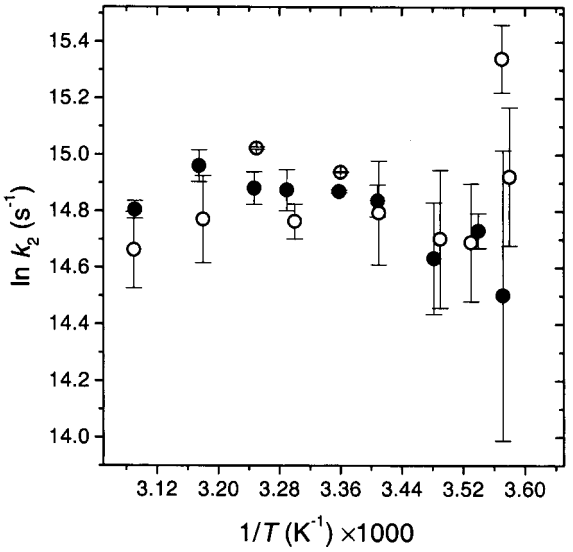

FIGURE 3 Arrhenius plot for the rate constant, k_2, of the $K_E \rightarrow K_L$ decay as measured by LIOAS in (○) DM-solubilized and (●) PML (20:1)-reconstituted pSRII-D75N. The decay is not thermally activated in the range 6.5–52°C. Error bars correspond to the dispersion of four independent experiments.

the photocycle returns completely to the parent compound, the efficiency of the second step should be $\eta = 1$ and then $\Phi_2 = \Phi_1 = 0.5$. Thus, $\Delta V_{R,2} = (\Delta V_{r,2}/\Phi_2) = (6.5 \pm 1)$ ml/mol (Table 2).

No significant differences were detected upon excitation of the sample with 500 and 532 nm. The smaller α value for 532 nm excitation (Table 1) is due to the smaller vibrational contribution to the detected heat with respect to excitation at 500 nm. Dilution of the protein to a higher PML to protein ratio (100:1) had negligible effects on the LIOAS results (Table 1).

LIOAS with detergent-solubilized protein

The $\varphi_1 E_\lambda$ versus $(c_p\rho/\beta)$ plots for the DM-solubilized protein are not linear in the whole temperature range used (6–50°C). A negative deviation from linearity was observed at $T > 20°C$ due to a change in the absorbance with temperature. At 50°C, up to 25% of the absorbance is lost at the maximum and converted to a form spectrally similar to deprotonated SB (see above), giving rise to underestimation of the LIOAS amplitudes. A correction for this effect affords linear plots (Fig. 4). This thermochromic effect is reversible and is related to the altered pK_a values of the SB in the DM preparation (see below) with respect to the PML sample. The fraction of energy released as heat in the first step is unity in DM, much larger than in PML. On the contrary, $\Delta V_{r,1}$ is the same for the two preparations. The second amplitude still is associated with an expansion, larger in DM ($\Delta V_{r,2} = 8.5 \pm 0.2$ ml/mol) than in PML, $\Delta V_{r,2} = (3.3 \pm 0.25)$ ml/mol, and corresponding to a similar lifetime $\tau_2 = (360 \pm 70)$ ns in both preparations.

Fluorescence

At variance with pSRII-WT, pSRII-D75N in PML exhibits a weak fluorescence which allows the determination of the energy level of the first excited state $E_{00} \approx 200$ kJ/mol (600 nm). The quantum yield of fluorescence is very low in PML ($\Phi_F < 10^{-3}$), whereas it is somehow enhanced in DM ($\Phi_F \approx 5\ 10^{-3}$). The fluorescence spectrum in both media is a mirror image of the absorption spectrum and the Stokes shift is ~150 nm (Fig. 5). The energy wasted as fluorescence, $(\Phi_F E_F/E_\lambda) \leq 4\ 10^{-3}$ (with E_F = average energy of the fluorescence emission) can be neglected, as assumed in Eq. 3, in view of the fact that it is much smaller than the experimental error of α_{th1}.

Quantum yield as determined by laser flash photolysis

The absorption maximum of the first optically detectable intermediate (K_{565}) in pSRII-D75N is 45 nm red shifted

TABLE 2 LIOAS parameters for the decay $K_E \rightarrow K_L$

	pSRII-D75N				pSRII-WT*		
	λ_{exc} (nm)	α_{th2}	$\Delta V_{r,2}$† (ml/mol)	$\Delta V_{R,2}$‡ (ml/mol)	α_{th2}	$\Delta V_{r,2}$† (ml/mol)	$\Delta V_{R,2}$‡ (ml/mol)
PML 20:1	532	0.13 ± 0.03	3.1 ± 0.2	6.1 ± 1.0			
PML 20:1	500	0.1 ± 0.03	3.2 ± 0.2	6.3 ± 1.0	0.2 ± 0.05	−2 ± 0.6	9.4 ± 1.5
PML 100:1	500	0.01 ± 0.01	3.6 ± 0.2	7.0 ± 1.1	0.25 ± 0.05	−1 ± 0.3	8.6 ± 0.8
DM	532	−0.03 ± 0.03	8.5 ± 0.2	16.7 ± 2.0	0.09 ± 0.04	5.6 ± 0.7	11 ± 2.4

K_E decays in pSRII-D75N with an average τ_2 = 400 ns, whereas K → L decay in pSRII-WT is thermally activated and τ_2 = 1 μs at room temperature. Note the opposite sign of $\Delta V_{r,2}$ for pSRII-WT in the membrane solutions.

*Losi et al. (1999b).

†Measured values. In every case the regression value of the linear fitting was $r > 0.990$.

‡Molar structural volume change calculated using $\Delta V_{r,i}$ and the quantum yields, as $\Delta V_{r,i/\Phi_i}$ and considering the relative errors.

with respect to that of the parent state (λ_{max} = 565 nm, ϵ_{565} = 43000 M^{-1} cm^{-1} (Schmies et al., 2000), i.e., the spectral overlap between parent compound and K is much less than in pSRII-WT (Chizov et al., 1998). This allows the direct monitoring of K_{565} formation at wavelengths where the absorption of the parent state is negligible. The molar absorption coefficient of K_{565} at 600 nm is estimated to be 30,000 M^{-1} cm^{-1} for PML-reconstituted pSRII-D75N. The comparative method was applied for the measurement of Φ_K, as described in van Brederode et al. (1995) (see also Bensasson et al., 1978). The values used for the TPPS reference were Φ_{TPPS} = 0.6 (Davila and Harriman, 1990) and $\epsilon_{460,TPPS}$ = 47,000 M^{-1} cm^{-1}, the absorption coefficient for the triplet-triplet absorption of TPPS (van Brederode et al., 1995). E_a is the laser energy per pulse, and $\Delta A/E_a$ is the slope of the absorbance change versus E_a, derived from the linear fluence-dependent region. For TPPS, the maximum amplitude was recorded 1 μs after the laser pulse, whereas for pSRII-D75N the values between 0.5 and 6 μs were averaged. The positive ΔA at 600 nm is, in fact, constant in this time scale (Fig. 6). Both compounds show sharp fluence linearity up to ~140 μJ/pulse. The comparison of $\Delta A/E_a$ for the sample at 600 nm and TPPS (two series of experiments at room temperature) yielded Φ_K = 0.51 ± 0.05.

Alternatively, the bleaching of the parent state at 510 nm in the same time region (Fig. 6) may be used together with the data for TPPS for the evaluation of Φ_K. At 510 nm, however, the absorption by the parent state and K_{565} must be taken into account. The molar absorption coefficient is $\epsilon_{510,K} \approx$ 15,000 M^{-1} cm^{-1} for K_{565}, that results in 34% absorption contribution ($\epsilon_{510,G}$ = 44000 M^{-1} cm^{-1} for the parent state). Applying a simplified treatment as in Losi et al. (1999a) (namely dividing by $[1 - \epsilon_{510,K}/\epsilon_{510,G}]$, Φ_K = 0.53 ± 0.05 is calculated, similar to the value derived from the absorbance increase at 600 nm. Because detergent-dissolved protein samples rapidly degraded, no flash photolysis measurements were carried out with the DM preparations.

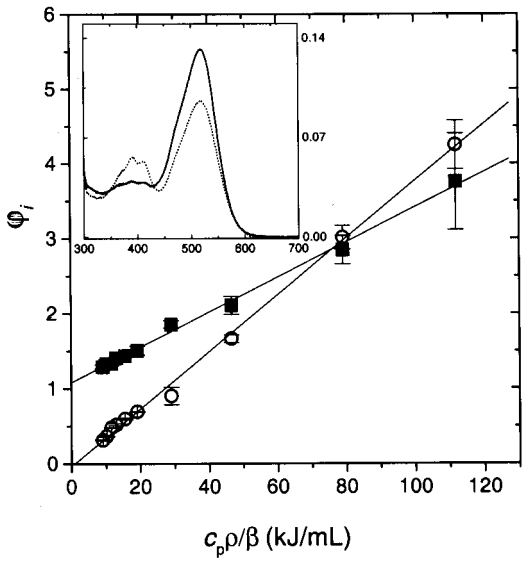

FIGURE 4 Plot of the LIOAS amplitudes associated with (■) formation and (○) decay of K_E in DM samples. The amplitudes were corrected for the temperature dependence of the absorbance at λ_{exc} = 532 nm. *Inset*: absorption spectra at (——) 20 and (- - - -) 52°C. The thermally induced optical change is completely reversible.

DISCUSSION

The mutation Asp-75 by the neutral residue Asn in PML-reconstituted pSRII-D75N affects neither the yield of the

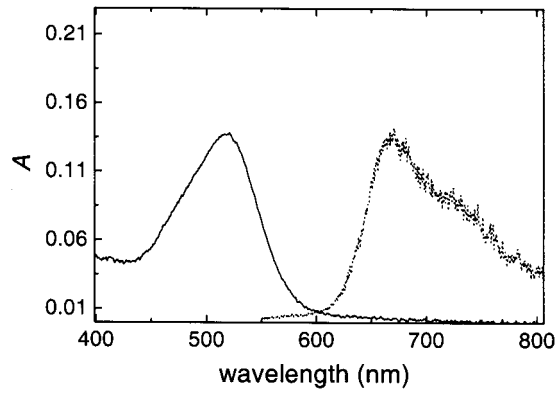

FIGURE 5 (——) Absorption and (- - - -) fluorescence spectrum of pSRII-D75N in DM. λ_{exc} = 510 nm, T = 6.5°C. The fluorescence spectrum was normalized to the absorption maximum.

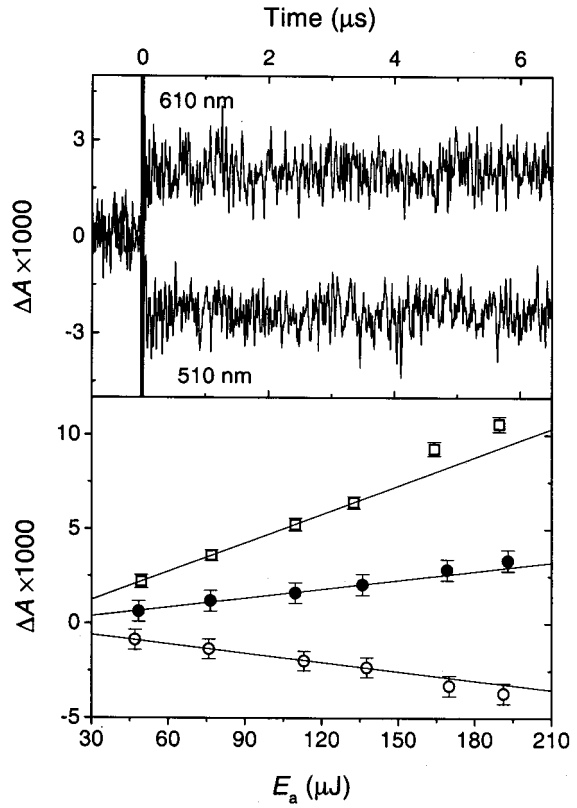

FIGURE 6 Flash photolysis determination of Φ_K in PML-reconstituted pSRII-D75N. *Top*: bleaching of the parent state at 510 nm (*bottom line*) and absorption of K_{565} at 610 nm. *Bottom*: plots of ΔA versus incident energy for (□), TPPS *T-T* absorption monitored as the amplitude at 460 nm immediately after the laser pulse; (●) formation of K_{565} in pSRII-D75N at 610 nm, and (○) bleaching of pSRII-D75N parent state at 510 nm. For pSRII-D75N, the average value of ΔA between 0.5 and 6 μs was taken. On this time scale, K_{565} appears as a permanent product (*top*). At the maximum fluence of 200 μJ, 2% of the molecules in the illuminated volume were photoconverted to K_{565} intermediate.

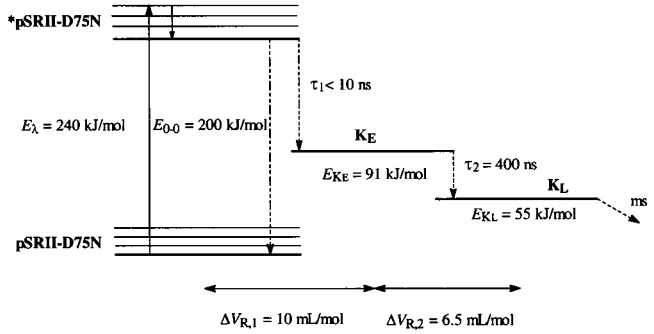

FIGURE 7 Enthalpy profile and structural volume changes for the early steps of the pSRII-D75N photocycle. The 400-ns decay of K_E is optically silent in our transient absorption experiment. K_L thermal decay is outside the LIOAS window. The 565 transient absorbance decay (Schmies et al., 2000) is attributed to the decay from K_E.

photochemical step (Φ_K = 0.51 ± 0.05 for pSRII-D75N and 0.5 ± 0.06 for pSRII-WT (Losi et al., 1999b), nor the energy stored in the first step occurring in the subnanosecond region with $\tau_1 < 10$ ns. Taking into account that, using step-scan FTIR for the study of the early steps of the BR photocycle, two K-type intermediates have been identified, an early one optically silent, K_E, and a later one, K_L, corresponding to K_{565} (Dioumaev and Braiman, 1997), we tentatively assign our 400-ns decay to the $K_E \rightarrow K_L$ transition in pSRII-D75N. Thus, we obtain a value E_{KE} = (91 ± 11) kJ/mol for pSRII-D75N versus E_K = (88 ± 13) kJ/mol for pSRII-WT. Also, similar conclusions concerning the energy level of the K intermediates were obtained for the corresponding BR-D85N (Logunov et al., 1996) and SRI-D76N (Losi et al., 1999a) and their wild-type counterparts. In analogy to the recent suggestion for the case of BR-D85N (Humphrey et al., 1997), also in pSRII-D75N, the first intermediate probably assumes a geometry that initiates a nonfunctional sequence. Its formation, however, is unperturbed by the mutation. An alternative explanation would be that the absence of the proper counterion inhibits the proton transfer from the otherwise similarly isomerized chromophore.

The value of $\Delta V_{R,1}$ (10 ± 0.3 for the mutant versus 9 ± 0.4 ml/mol for pSRII-WT) is also not significantly affected by the absence of a negative charge on this residue (Table 1), suggesting that similar molecular movements are triggered by isomerization in pSRII-WT and in pSRII-D75N and that Asp-75 plays an important role only in the conformational changes occurring later in the photocycle. Quite interestingly, $\Delta V_{R,1}$ is significantly different for SRI-WT (5.5 ml/mol) and for SRI-D76N (1.5 ml/mol), though the mutation should not alter the charge pattern in the retinal cavity. We should thus conclude that the charge on this residue is not a major factor in determining the magnitude of $\Delta V_{R,1}$.

Again in analogy to the recent speculation about the role of Asp-85 in BR (Pebay-Peyroula et al., 1997), it is possible that the protonated SB in pSRII and Asp-75 are not hydrogen bonded in the parent state, and that they establish a connection only when K relaxes into the L state (reviewed in Oesterhelt, 1998). In agreement with this hypothesis, the subsequent steps are markedly influenced by the D75N mutation.

K decays into L with a lifetime of 1 μs at room temperature in PML-reconstituted pSRII-WT. This relaxation is accompanied by a contraction of 3 ml/mol (Losi et al., 1999b). L is not formed and K_{565} lives at least 7 ms at room temperature in pSRII-D75N (Schmies et al., 2000). In pSRII-WT, we do not observe a biphasic decay of K. Our LIOAS data for pSRII-D75N show that K_E, bearing the isomerized chromophore, is formed within $\tau_1 < 10$ ns, which agrees with our flash photolysis data (Fig. 6, upper panel). K_E decays with τ_2 = 400 ± 120 ns, showing an expansion. This decay is optically silent, i.e., it was not

optically detected in our transient absorption experiments (Fig. 6) indicating that no back isomerization takes place within this time. The deactivation should thus occur through a coupling of the chromophore excess energy with protein vibrations not affecting the chromophore conjugation. A support for this hypothesis is the lack of activation of this decay (Fig. 3). The return of K_{565} back to the ground state (isomerization and protein relaxation) takes place in the long ms time scale (outside our LIOAS time window) as determined by transient absorption spectroscopy (Schmies, 2000).

Concerning the free energy profile (Fig. 7), the formation of K_E in the mutated protein is driven by the same free energy as in pSRII-WT, i.e., $\Delta G_K = -40$ kJ/mol. The thermodynamics of formation and biphasic decay of K_E is calculated as explained below.

Because, most probably, hydrogen bonds influence the chromophore–protein interactions during this decay, we assume the relation $T\Delta S_{R,i} = X\,\Delta V_{R,i}$. with $X = 13$ kJ/mL established for reactions in aqueous solutions with compounds displaying strong hydrogen bonds (Borsarelli and Braslavsky, 1999). Thus, the structural volume change upon formation of K_L is $\Delta V_{K_l} = \Delta V_{R,1} + \Delta V_{R,2} = (10 + 6.5)$ ml/mol and $T\Delta S_{K_L} = (216 \pm 40)$ kJ/mol. With the value of $E_{K_L} = (55 \pm 30)$ kJ/mol, we obtain $\Delta G_{R,K_L} \sim -160$ kJ/mol for the free energy of K_L production. This intermediate thus plays the role of a "free energy trap" in the pSRII-D75N photocycle, explaining its unusually long lifetime. The large error in the E_{K_L} value is due to the large uncertainty in the value of α_2.

Finally, we underline the strong effects of the solubilizing medium (PML versus detergent) on some physico-chemical parameters such as the pK_a of the SB, the stability toward high pH (Fig. 1), the fluorescence quantum yield, and the amount of energy released as heat (Table 1). The differences between the values for pSRII-WT in the two media are not so striking, showing that the counteranion Asp-75 has a stabilizing effect. Nevertheless, the pK_a value of Asp-75 was determined for pSRII-WT as 3.5 in DM and 5.6 in PML, suggesting that the interaction of pSRII-WT with the detergent exposes other carboxyl groups, thereby contributing to the protonation mechanism of the counterion complex (Chizov et al., 1998). Furthermore, in pSRII-WT the decay of K into L corresponds to an expansion in DM and to a contraction in PML, indicating a different exposure of the active site to the solvent or a different conformation of the protein in this stage of the photocycle (Losi et al., 1999b). We note that protein–protein interactions in pSRII-WT could be detected by electron spin resonance only in the PML samples, but not in the DM solubilized form (A. A. Wegener, unpublished results). The effects of the solubilizing medium on the structure and properties of retinal proteins (and photocycle intermediates) is certainly a subject of outstanding interest, which needs further examination.

A. Losi was supported by the Marie Curie grant #ERBFMBICT972377. The able technical assistance by Gudrun Klihm and Dagmar Lenk is greatly appreciated. We are indebted to Professor Kurt Schaffner for his continuous generous support.

REFERENCES

Bensasson, R., C. R. Goldschmidt, E. J. Land, and T. G. Truscott. 1978. Laser intensity and the comparative method for determination of triplet quantum yields. *Photochem. Photobiol.* 28:277–281.

Bogomolni, R. A., W. Stoeckenius, I. Szundi, E. Perozo, K. D. Olson, and J. L. Spudich. 1994. Removal of transducer HtrI allows electrogenic proton translocation by sensory rhodopsin I. *Proc. Natl. Acad. Sci. USA.* 91:10188–10192.

Borsarelli, C. D., and S. E. Braslavsky. 1999. Enthalpy, volume, and entropy changes associated with the electron transfer reaction between the ^{3}MLCT state of $Ru(bpy)_3^{2+}$ and methylviologen cation in aqueous solutions. *J. Phys. Chem. A.* 103:1719–1727.

Braslavsky, S. E., and G. E. Heibel. 1992. Time-resolved photothermal and photoacoustic methods applied to photoinduced processes in solution. *Chem. Rev.* 92:1381–1410.

Chizov, I., G. Schmies, R. Seidel, J. R. Sydor, B. Lüttenberg, and M. Engelhard. 1998. The photophobic receptor from *Natronobacterium pharaonis*: temperature and pH dependencies of the photocycle of sensory rhodopsin II. *Biophys. J.* 75:999–1009.

Davila, J., and A. Harriman. 1990. Photoreactions of macrocyclic dyes bound to human serum albumin. *Photochem. Photobiol.* 51:9–19.

Dioumaev, A. K., and M. S. Braiman. 1997. Two bathointermediates of the bacteriorhodopsin photocycle, distinguished by nanosecond time-resolved FTIR spectroscopy at room temperature. *J. Phys. Chem. B.* 101:1655–1662.

Edman, K., P. Nollert, A. Royant, H. Berlhali, E. Pebay-Peyroula, J. Hajdu, R. Neutze, and E. M. Landau. 1999. High-resolution x-ray structure of an early intermediate in the bacteriorhodopsin photocycle. *Nature.* 401: 822–826.

Engelhard, M., B. Scharf, and F. Siebert. 1996. Protonation changes during the photocycle of sensory rhodopsin II from *Natronobacterium pharaonis. FEBS Lett.* 395:195–198.

Gensch, T., J. M. Strassburger, W. Gärtner, and S. E. Braslavsky. 1998. Volume and enthalpy changes upon photoexcitation of bovine rhodopsin derived from optoacoustic studies by using an equilibrium between bathorhodopsin and blue-shifted intermediate. *Israel J. Chem.* 38: 231–236.

Hage, W., M. Kim, H. Frei, and R. A. Mathies. 1996. Protein dynamics in the bacteriorhodopsin photocycle: a nanosecond step-scan FTIR investigation of the KL to L transition. *J. Phys. Chem.* 100:16026–16033

Haupts, U., E. Bamberg, and D. Oesterhelt. 1996. Different modes of proton translocation by sensory rhodopsin I. *EMBO J.* 15:1834–1841.

Humphrey, W., E. Bamberg, and K. Schulten. 1997. Photoproducts of bacteriorhodopsin mutants: a molecular dynamics study. *Biophys. J.* 72:1347–1356.

Logunov, S. L., M. A. El-Sayed, L. Song, and J. K. Lanyi. 1996. Photoisomerization quantum yield and apparent energy content of the K intermediate in the photocycles of bacteriorhodopsin, its mutants D85N, R82Q, and D212N, and deionized blue bacteriorhodopsin. *J. Phys. Chem.* 100:2391–2398.

Losi, A., S. E. Braslavsky, W. Gärtner, and J. Spudich. 1999a. Time-resolved absorption and photothermal measurements with sensory rhodopsin I from *Halobacterium salinarum. Biophys. J.* 76:2183–2191.

Losi, A., A. A. Wegener, M. Engelhard, W. Gärtner, and S. E. Braslavsky. 1999b. Time-resolved absorption and photothermal measurements with recombinant sensory rhodopsin II from *Natronobacterium pharaonis. Biophys. J.* 77:3277–3286.

Mogi, T., L. J. Stern, T. B. Marti, B. H. Chao, and H. G. Khorana. 1988. Aspartic acid substitutions affect proton translocation by bacteriorhodopsin. *Proc. Natl. Acad. Sci. USA.* 85:4148–4152.

Oesterhelt, D. 1998. The structure and mechanism of the family of retinal proteins from halophilic bacteria. *Curr. Opinion Struct. Biol.* 8:489–500.

Pebay-Peyroula, E., G. Rummel, J. P. Rosenbusch, and E. M. Landau. 1997. X-ray structure of bacteriorhodopsin at 2.5 Angstroms from microcrystals grown in lipid cubic phases. *Science.* 277:1676–1681.

Rath, P., K. D. Olson, J. L. Spudich, and K. J. Rothschild. 1994. The Schiff base counterion of bacteriorhodopsin is protonated in sensory rhodopsin I—spectroscopic and functional characterization of the mutated proteins D76N and D76A. *Biochemistry.* 33:5600–5606.

Ruddat, A., P. Schmidt, C. Gatz, S. E. Braslavsky, W. Gärtner, and K. Schaffner. 1997. Recombinant type A and B phytochromes from potato. Transient absorption spectroscopy. *Biochemistry.* 36:103–111.

Rudzki-Small, J., L. J. Libertini, and E. W. Small. 1992. Analysis of photoacoustic waveforms using the nonlinear least square method. *Biophys. Chem.* 41:29–48.

Rudzki, J. E., J. L. Goodman, and K. S. Peters. 1985. Simultaneous determination of photoreaction dynamics and energetics using pulsed, time-resolved photoacoustic calorimetry. *J. Am. Chem. Soc.* 107: 7849–7854.

Schmies, G., B. Lüttenberg, I. V. Chizhov, M. Engelhard, A. Becker, and E. Bamberg. 2000. Sensory rhodopsin II from the haloalkaliphilic *Natronobacterium pharaonis*: Light-activated proton transfer reactions. *Biophys. J.* 78:967–976.

Schulenberg, P., and S. E. Braslavsky. 1997. Time-resolved photothermal studies with biological supramolecular systems. *In* Progress in Photothermal and Photoacoustic Science and Technology. Vol 3. Life and Earth Sciences. A. Mandelis and P. Hess, editors. SPIE, Bellingham, WA. 58–81.

Siebert, F. 1995. Application of FTIR spectroscopy to the investigation of dark structures and photoreactions of visual pigments. *Israel J. Chem.* 35:309–323.

Spudich, E. N., W. S. Zhang, M. Alam, and J. L. Spudich. 1997. Constitutive signaling by the phototaxis receptor sensory rhodopsin II from disruption of its protonated Schiff base Asp-73 interhelical salt bridge. *Proc. Natl. Acad. Sci. USA.* 94:4960–4965.

Subramaniam, S., D. A. Greenhalgh, and H. G. Khorana. 1992. Aspartic acid 85 in Bacteriorhodopsin functions both as proton acceptor and negative counterion to the Schiff base. *J. Biol. Chem.* 267:25730–25733.

van Brederode, M. E., T. Gensch, W. D. Hoff, K. J. Hellingwerf, and S. E. Braslavsky. 1995. Photoinduced volume change and energy storage associated with the early transformations of the photoactive yellow protein from *Ectothiorhodospira halophila. Biophys. J.* 68:1101–1109.

Weidlich, O., and F. Siebert. 1993. Time-resolved step-scan FT-IR investigations of the transition from KL to L in the bacteriorhodopsin photocycle: Identification of chromophore twists by assigning hydrogen-out-of-plane (HOOP) bending vibrations *Appl. Spectrosc.* 47: 1394–1400.

Zhang, H., and D. Mauzerall. 1996. Volume and enthalpy changes in the early steps of bacteriorhodopsin photocycle studied by time-resolved photoacoustics. *Biophys. J.* 71:381–388.

Zhu, J., E. N. Spudich, M. Alam, and J. L. Spudich. 1997. Effects of substitutions D73E, D73N, D103N, and V106M on signaling and pH titration of sensory rhodopsin II. *Photochem. Photobiol.* 66:788–791.